Pt and TCO free hybrid bilayer silver nanowire−graphene counter electrode for dye-sensitized solar cells

Mohammad Al-Mamun[a], Jae-Yup Kim[b], Yung-Eun Sung[c], Jae-Joon Lee[d], Sung-Ryong Kim[a,*]

[a]Department of Polymer Science and Engineering, Korea National University of Transportation, Chungju 380-702, Republic of Korea.

[b]Fuel Cell Center, Korea Institute of Science and Technology (KIST), Seoul 136-791, Republic of Korea.

[c]School of Chemical & Biological Engineering, Seoul National University, San 56-1, Sillim-dong, Gwanak-gu, Seoul 151-742, Republic of Korea.

[d]Department of Applied Chemistry, Konkuk Univ, 322 Danwol-dong, Chungju 380-701, Republic of Korea.

Abstract

Here we report a novel transparent conductive oxide (TCO) and Pt free silver nanowire and graphene nanoplatelet (AgNW-GNP) based hybrid counter electrode (CE) for dye-sensitized solar cells (DSSCs) having appreciable photovoltaic performances compared to reference Pt-FTO based DSSCs. Simple solution processed bilayer AgNW-GNP hybrid CEs were prepared to investigate its applicability in DSSCs based on their electrocatalytic and charge transport properties. DSSCs prepared with AgNW-GNP hybrid CEs containing the GNP loading of 0.88 μg/cm^2 showed the photoconversion efficiency of 1.61±0.13 % which is comparable with that of 1.87±0.15 % made of standard Pt-FTO CEs.

Key words: Graphene nanoplatelets, Silver nanowire, Counter electrode, DSSCs, Tafel polarization

* Corresponding author. Tel.: +82 43 8415426; Fax: +82 43 8415420

E-mail address: srkim@ut.ac.kr (Sung-Ryong Kim)

1. Introduction

Dye-sensitized solar cells (DSSCs) are considered to be one of the most attractive alternative photovoltaics of solid-state silicon solar cells due to their potential to generate electricity on resource-abundant raw materials and energy-saving device processing [1,2]. A typical DSSC consists of transparent conducting oxide (TCO) films on a glass substrate, a wide band gap semiconductor, a ruthenium based dye, a redox electrolyte solution and a Pt coated TCO counter electrode (CE) [3]. The working mechanism of DSSCs accompanied by the ultrafast injection of photoelectron from the excited dye to the conduction band of semiconductor and the photoelectron pass through the external circuit to the CE [4]. The CE permits the catalytic reduction of oxidized electrolyte for the regeneration of sensitized dye [5]. Traditionally, Pt coated TCO glass is highly used as a CE due to its unique electrocatalytic property and exceptional stability under wide variety of redox shuttle [6]. The use of platinum as cathode material on TCO substrate accounts for more than 40% of the total device cost of a complete DSSC [7]. Therefore, tremendous efforts have been made to replace Pt with low-cost alternative materials to reduce the overall cost of DSSCs.

Different types of carbonaceous material like activated carbon black[8], carbon nanotubes [9] , graphene nanoplatlets [10], functionalized graphene [11], graphene Au NPs composite [12], reduced graphene oxide [13], and nickel phosphide-embedded graphene [14] were introduced as cathode materials in DSSCs. Recently, transition metal carbide, nitride and oxides showed promising replacement for Pt having competitive photoconversion efficiency (PCE) [15]. Several attempts were also made to replace Pt by conducting polymer like PEDOT:PSS[16] , polyaniline [17] and polypyrrole [18].

However, most of the Pt-free cathode materials in DSSCs were tested on an expensive TCO substrate to facilitate the sufficient charge transport for the completion of the total circuit. In order to replace Pt and TCO substrate simultaneously, highly conductive PEDOT films prepared by in-situ polymerization on a plain glass were reported as an effective CE for DSSCs [19]. Sub-micrometer-sized graphite films on a glass were also reported as conducting catalytic CE with maintaining thickness of several micrometers which may not be beneficial for large scale production of DSSCs [20]. There is only one report on the silver nanowire (AgNW) based CEs for solid state DSSCs [21].

In this work, we firstly applied the AgNW as a catalytic CE in DSSCs. The sparse network of nanowires resulted in open spots in the entire film. It is speculated that these open spots are responsible for the poor catalytic property and hinder the charge transportation throughout the film. To compensate such kind of poor electrocatalytic conversion of cobalt ion in the liquid type electrolyte along with facilitating the electrical tunneling pathway, we applied graphene nanoplatelets (GNP) over AgNW film. The introduction of GNP over AgNW film resulted in significant improvement of electrocatalytic property in cobalt based mediator electrolyte. This hybrid bi-layer conducting catalytic counter electrodes on a plain glass showed comparable PCEs with the reference Pt-FTO CE based DSSCs.

2. Experimental

Silver nanowires (AgNW) having the diameter ranging from 40-70 nm with the aspect ratio of ~200 were synthesized according to the procedure reported elsewhere [22]. AgNW conducting films were prepared on plain glass substrate by drop casting of AgNW dispersion in isopropyl alcohol with maintaining the mass loading of 0.59 μg/cm^2. Prior to AgNW drop casting, the glass substrates were treated by $H_2O_2/NH_3.H_2O$ and functionalized by (3-aminopropyl) triethoxysilane to improve the adhesion between the wires and substrate. On

the other hand, graphene nanoplatelets (GNP) (xG Science, Grade C-750 m^2/g) consists of several sheets of graphene with an overall thickness of ~5 nm (ranging from 1 to 15 nm) and the particle diameter of ~220 nm as shown in Figure S1 were used to prepare the concentration of 2.0 mg/mL. Firstly, the dispersion was centrifuged at 7000 rpm to remove the larger platelets and the supernatant containing a few layer of graphene was collected. The final dispersion was stable for several days without any marked sedimentation. The GNP dispersion was spin coated on previously prepared AgNW film at 500−1000 rpm and thermally annealed at 150 °C for 20 min. Figure 1 shows the schematic illustration of silver nanowire and bilayer hybrid silver nanowire-graphene nanoplatelets based counter electrodes (CEs). The mass loadings of GNP ranging from 0.29−1.48 $\mu g/cm^2$ were controlled by varying the spin speed and number of spin-coating. Sheet resistance measurements were executed by automatic mapping four point probe system (CMT-SR2000N, Materials Development Corp.).

Cobalt redox couples, i.e., $Co^{3+/2+}$ tris(4,40-di-*tert*-butyl-2,20-bipyridyl) {$[Co(t\text{-}Bu_2bpy)_3]^{3+/2+}$}, were synthesized according to our previous paper [23]. The final electrolyte consisted of 0.22 M $[Co(t\text{-}Bu_2bpy)_3]^{3+/2+}$, 0.20 M $LiClO_4$ (Aldrich, 99.99%), 0.20 M 4-tertbutylpyridine (Aldrich, 96%), and 0.02 M $NOBF_4$ (Aldrich, 95%), in acetonitrile. TiO_2 (Ti-Nanoxide D, Solaronix SA) film thickness of ~8 µm was sensitized by ruthenium sensitizer (N719, Solaronix SA) and assembled with the predrilled modified (CEs) by using a Surlyn® spacer. Then few drops of cobalt complex electrolyte were injected into the cell. Platinum target (Ø 57 mm×0.1 mm; 99.95% Pt; Cressington; England) was sputtered on the pre-cleaned FTO-glass substrate using a sputter coater (Cressington Sputter Coated 108 auto, Cressington Scientific Instruments Ltd., England) under argon atmosphere at the operating current of 10 mA and the deposition time was 200 s. These Pt sputtered FTO-glass was considered as reference CEs for comparison.

Cyclic voltammograms (CVs) were recorded using Autolab PGSTAT12 (the Netherlands) in the voltage range of -0.40 to 0.60 V (with respect to a saturated Ag/Ag^{+} reference electrode) at a scan rate of 100 mV/s in a three electrode configuration. The diluted electrolyte for CV measurements consisted of 2.2 mM Co^{3+} complex, 0.2 mM $NOBF_4$ and 0.1 M $LiClO_4$ in acetonitrille. A Pt wire was used as counter electrode. The DSSCs were illuminated under 100 mW/cm^2, AM 1.5 using a 450 W Xe high power arc lamp housing (LH 151, Spectral Energy Co.). The light intensity was calibrated using a Radiometer Photometer (ILT 1400-A, International Light Technologies Inc.). A symmetrical dummy cell, consisting of two identical glasses coated with the catalytic materials with the active are of 1.0 cm^2 were sealed. The distance between the electrodes was ~73 μm. These dummy cells containing the same operating electrolyte used for DSSCs were used for measuring electrochemical impedance spectroscopic (EIS) and Tafel polarization measurements. The EIS experiments were carried out with an impedance analyzer (CH Instruments, Inc.). The frequency range was 10^5–10^{-1} Hz and the perturbation amplitude was 10 mV. All measurements were performed at room temperature in the dark condition at 0 V. A ZView software (Scribner Associates Inc.) was used to process the EIS data. Tafel polarization measurements were carried out with an electrochemical workstation (CH Instruments, Inc.) with the scan rate of 10 mV/s.

3. Results and discussion

Figure 2 shows the surface morphology of silver nanowire (AgNW) and silver nanowire-graphene nanoplatelets (AgNW-GNP) on glass substrate which indicated the dense coverage of glass substrate to achieve reasonable charge transport capability. Even after the dense coverage of AgNW, there were some uncovered spots as large as ~2 μm due to the sparse network of AgNWs. Graphene nanoplatelets (GNP) were coated on AgNW film as

shown in Figure 2b and the bilayered surface was shown to have homogeneous coverage along with a significant decrease of surface roughness from the initial value of 36.41 to 25.11 nm (Figure 2c and Figure 2d). The significant decrease of surface roughness could be related to the coverage by GNP as shown in Figure 1. The cross-sectional image (Figure 2b) showed the thickness of the AgNW layer of ~516 nm which corresponds to ~6 nanowires. AgNW film layer was tightly sandwiched between glass substrate and over-coated GNP. The sheet resistance of AgNW film was measured using four-probe technique at 9 different locations of 9 cm^2 film and the average value was 1.64 Ω/□ as shown in Figure S2.

The catalytic properties and reaction kinetics of different types of electrodes were investigated by cyclic voltammetric (CV) measurements. The comparative cyclic voltammograms (CVs) obtained from different types of electrodes were plotted in Figure 3a. A well defined redox peaks were observed for Pt-FTO electrode, whereas AgNW electrode indicated an ill-defined redox peaks without any distinguishable peaks due to the insufficient reduction of Co^{3+} species in the electrolyte. On the other hand, the GNP over-coated electrodes were shown to have higher current density with traces of redox peaks compared to AgNW only. AgNW-GNP3 showed the highest cathodic current out of hybrid electrodes possessing over-coated GNP layer. The GNP layer would provide larger interfacial surface area with cobalt redox electrolyte, resulting in moderate catalytic activity. The smaller current and indistinguishable peaks of AgNW-GNP4 electrodes compared to Pt-FTO could be related to the slow charge transfer process involving $Co^{2+/3+}$ couple. The large inner sphere reorganization energy of cobalt complex and high scan rate (100 mV/s) during CV measurement could be the other reasons for getting indistinguishable cathodic peaks for hybrid electrodes [24].

Figure 3b shows the impedance spectra obtained for the symmetric cells with different types of CEs. The obtained data were fitted by an equivalent circuit analogue in Figure 3b (inset). The semicircle in the high frequency regime is related to the charge transfer resistance (R_{ct}) between CE and cobalt redox mediator. The semicircle in low frequency range is related with the resistance of electrolyte diffusion (Z_w). Each of the parameters is listed in Table 1. The trends of the R_{ct} are in good agreement with catalytic activity observed by CV measurement. The AgNW-GNP3 showed the lowest R_{ct} value among CEs. The Z_w of AgNW and AgNW-GNP was several times higher than that of Pt. Unlike the iodide redox mediator, the cobalt redox mediator cannot penetrate through the mesoporous film smoothly due to the relatively larger volume of the complex [23]. The Pt sputtered CE has a flat surface; however, the AgNW and AgNW-GNP based CEs have a porous structure. Therefore, the Z_w value of AgNW and AgNW-GNP could be higher than that of Pt. The ohmic serial resistance, R_s, was higher than standard Pt-FTO which indicated the poor contact between AgNW and GNP compared to Pt-FTO.

Further investigations on the electrocatalytic properties of the prepared electrodes were conducted by measuring Tafel polarization curves and presented in Figure 3c. The exchange current density, J_o, was obtained from the intercept of the extrapolated linear region of the curve when the over potential is zero [25]. A comparable cathodic slope was found in the symmetrical cells for AgNW-GNP3 electrode which showed its catalytic activity towards the reduction of Co^{3+} to Co^{2+}. The variation of J_o, obtained from Tafel polarization measurement is closely associated with the R_{ct} value as shown in eqn (1) [15].

$$J_o = \frac{RT}{nFR_{ct}} \tag{1}$$

where, R is the gas constant, T is the temperature, F is Faraday's constant, n is the number electrons involving in the reaction, and R_{ct} is the charge transfer resistance. The tendency of R_{ct} variation in Table 1 with J_o of different electrodes is in good agreement with the relation in eqn (1). It should be noted that the limiting current density, J_{lim}, has a positive relation with the diffusion coefficient and the diffusion coefficient is also correlated negatively with the diffusion impedance, Z_w [15]. After performing the comprehensive analysis of CV, EIS and Tafel polarization results, we conclude that the TCO free hybrid CEs made of AgNW and GNP show reasonable catalytic activity compare to Pt-FTO in cobalt mediator based DSSCs.

Figure 4a presents the IPCE spectra of the DSSCs with different counter electrodes. The IPCE spectra were measured as a function of wavelength from 400 to 800 nm using a specially designed IPCE measurement system (PV Measurements, Inc.) for DSSCs. The DSSCs with TCO-free AgNW-GNP counter electrode showed comparable external quantum efficiency to Pt-FTO electrode over the whole spectral range of incident light.

The *J-V* characteristics of the devices with Pt-FTO, AgNW and two different AgNW-GNP based hybrid CEs with a different GNP loading are shown in Figure 4b. Under illumination, Pt-FTO based reference DSSC exhibited a J_{sc} of 6.47 mA/cm^2, a V_{oc} of 0.58 V, a fill factor of 0.44 and an overall conversion efficiency of 1.87 %. The DSSC with AgNW-GNP3 hybrid CE having the GNP loading of 0.88 μg/cm^2 showed the highest fill factor (*FF*) of 0.52 and a J_{sc} of 6.45 mA/cm^2, a V_{oc} of 0.55 V, and a photoconversion efficiency (PCE) of 1.61 %, which is comparable to using Pt-FTO electrode. The photovoltaic performances of the different CEs are summarized in Table 2, where the average values were obtained from at least three different cells. The possible reason for the superior photovoltaic performance of AgNW-GNP based DSSCs compared to AgNW only could be related to the accessible catalytic sites created by GNP [26]. However, the conversion efficiencies of DSSCs based on

AgNW-GNP counter electrodes were dependent on the amount of GNP loading in the hybrid CEs. We speculate that the further increase of GNP loading (> 0.88 μg/cm^2) would increase the interfacial charge transfer resistance (R_{ct}) between the GNP flakes, therefore, slower electron diffusion and transport, high charge recombination and low conversion efficiency [27]. In addition, higher GNP loading could severely shield the light harvesting of the sensitizer and the number of photo-generated electrons would also decrease under illumination.

It is important to mention that the trend of electrocatalytic activity and R_{ct} among AgNW and AgNW-GNP are closely related to *FF* and conversion efficiency. It is also worthwhile to mention that the DSSCs under the combination of N719 (Ruthenizer 535-bisTBA) as a sensitizer and cobalt bipyridal complex ([Co(t-Bu2bpy)3]n+) as a redox couple exhibited relatively lower photo conversion efficiency compared to I3-/I- based electrolyte
[23,24,28]. Typically, cobalt bipyridal complex is reported to possess some inferior properties such as slower dye reduction, faster recombination with photoinjected electrons and slower diffusion [29]. Specially, the large size of the cobalt bipyridal complex leads to insufficient mass transport of the oxidized species through the mesoporous electrode which limit the photocurrent and hereby lower the photovoltaic performances in DSSCs [30]. On the other hand, iodide electrolyte based DSSC showed comparatively higher photo-conversion efficiency ca. 6.01 % with standard Pt-FTO based CE as shown in Figure S3. Although the absolute efficiency values were somewhat low, due to the unfavorable combination of conventional N719 sensitizer with cobalt redox mediator system but the suitable coupling between sensitizer and cobalt electrolyte would provide higher photo conversion efficiency. However, this study clearly showed the application of AgNW-GNP based hybrid bilayer conducting counter electrode which could be an efficient alternative to the traditional Pt-TCO based CE for cobalt redox mediator based DSSCs.

4. Conclusions

Low-cost and easier fabrication method is demonstrated to prepare hybrid bilayer silver nanowire-graphene counter electrodes for cobalt mediator based DSSCs. The proposed CEs showed comparable electrocatalytic activity which was confirmed by cyclic voltammetry, electrochemical impedance spectroscopy and Tafel polarization measurements. The transparent conductive oxide free (TCO-free) CE of DSSCs resulted in ca. 86 % of photo conversion efficiency compared to the reference Pt-FTO CE. This work provides an effective alternative route to the expensive and scarce Pt and TCO for low cost DSSCs. The electrochemical property of AgNW-GNP based hybrid counter electrode can be further improved, which may give rise to the innovative thoughts for the simultaneous replacement of Pt and TCO in DSSCs.

Acknowledgements

This research was financially supported through the Human Resource Training Project for Regional Innovation by the Ministry of Education, Science Technology of Korea. Also, this work was supported by a grant 2010-0006808 of National Research Foundation of Korea Government. The authors would like to thank Professor Jae-Jung Ko, Korea University, for providing IPCE measurement facility and Mr. Kyung-Jae Lee, Seoul National University, for synthesizing the electrolyte.

References

[1] B. O'Regan, M. Gratzel. Nature. 353 (1991) 737.

[2] P. Wang, S.M. Zakeeruddin, P. Comte, I. Exnar, M. GrÃ¤tzel. J. Am. Chem. Soc. 125 (2003) 1166.

[3] S. Kim, M. Al-Mamun, Y. Ko. Chemical Physics Letters. 538 (2012) 77.

[4] A. Kay, M. GrÃ¤tzel. Chem. Mater. 14 (2002) 2930.

[5] K.S. Lee, W.J. Lee, N. Park, S.O. Kim, J.H. Park. Chem. Commun. 47 (2011) 4264.

[6] T.N. Murakami, M. Grätzel. Inorg. Chim. Acta. 361 (2008) 572.

[7] J. Lin, J. Liao, T. Wei. Electrochemical and Solid-State Letters. 14 (2011) D41.

[8] G.R. Li, F. Wang, J. Song, F.Y. Xiong, X.P. Gao. Electrochim. Acta. 65 (2012) 216.

[9] G.I. Lee, N.C.D. Nath, S. Sarker, W.H. Shin, A.J.S. Ahammad, J.K. Kang, J. Lee. Phys. Chem. Chem. Phys. 14 (2012) 5255.

[10] L. Kavan, J. Yum, M.K. Nazeeruddin, M. GrÃ¤tzel. ACS Nano. 5 (2011) 9171.

[11] J. Roy-Mayhew, D.J. Bozym, C. Punckt, I.A. Aksay. ACS Nano. 4 (2010) 6203.

[12] M. Al-Mamun, J. Lim, Y. Sung, S. Kim. Chem. Lett. 42 (2013) 31.

[13] H. Zheng, C.Y. Neo, X. Mei, J. Qiu, J. Ouyang. J. Mater. Chem. 22 (2012) 14465.

[14] Y.Y. Dou, G.R. Li, J. Song, X.P. Gao. Phys. Chem. Chem. Phys. 14 (2012) 1339.

[15] M. Wu, X. Lin, Y. Wang, L. Wang, W. Guo, D. Qi, X. Peng, A. Hagfeldt, M. GrÃ¤tzel, T. Ma. J. Am. Chem. Soc. 134 (2012) 3419.

[16] H. Shin, S.S. Jeon, S.S. Im. Synth. Met. 161 (2011) 1284.

[17] Q. Tai, B. Chen, F. Guo, S. Xu, H. Hu, B. Sebo, X. Zhao. ACS Nano. 5 (2011) 3795.

[18] J. Xia, L. Chen, S. Yanagida. J. Mater. Chem. 21 (2011) 4644.

[19] K.S. Lee, H.K. Lee, D.H. Wang, N. Park, J.Y. Lee, O.O. Park, J.H. Park. Chem. Commun. 46 (2010) 4505.

[20] G. Veerappan, K. Bojan, S. Rhee. ACS Appl. Mater. Interfaces. 3 (2011) 857.

[21] B.E. Hardin, W. Gaynor, I. Ding, S. Rim, P. Peumans, M.D. McGehee. Organic Electronics. 12 (2011) 875.

[22] L. Hu, H.S. Kim, J. Lee, P. Peumans, Y. Cui. ACS Nano. 4 (2010) 2955.

[23] J. Kim, K.J. Lee, S.H. Kang, J. Shin, Y. Sung. J. Phys. Chem. C. 115 (2011) 19979.

[24] S.A. Sapp, C.M. Elliott, C. Contado, S. Caramori, C.A. Bignozzi. J. Am. Chem. Soc. 124 (2002) 11215.

[25] L. Wang, E.W. Diau, M. Wu, H. Lu, T. Ma. Chem. Commun. 48 (2012) 2600.

[26] R. Bajpai, S. Roy, P. Kumar, P. Bajpai, N. Kulshrestha, J. Rafiee, N. Koratkar, D.S. Misra. ACS Appl. Mater. Interfaces. 3 (2011) 3884.

[27] J. Fan, S. Liu, J. Yu. J. Mater. Chem. 22 (2012) 17027.

[28] F. Ghamouss, R. Pitson, F. Odobel, M. Boujtita, S. Caramori, C. A. Bignozzi , Electrochim. Acta. 55 (2010) 6517.

[29] M.J. DeVries, M.J. Pellin, J.T. Hupp. Langmuir. 26 (2010) 9082.

[30] B.M. Klahr, T.W. Hamann. J. Phys. Chem. C. 113 (2009) 14040

Table 1

Electrochemical parameters from EIS and Tafel measurements for Pt-FTO, AgNW, AgNW-GNP3 and AgNW-G4 counter electrodes.

CEs	GNP-loading ($\mu g/cm^2$)	R_s (Ω)	R_{ct} ($\Omega\ cm^2$)	CPE:B ($\mu F/cm^2$)	Z_w ($\Omega\ cm^2$)	J_o (mA/cm^2)
Pt-FTO	–	15.37	16.47	138.78	17.91	44.67
AgNW	–	71.88	47.73	44.38	120.15	10.47
AgNW-GNP3	0.88	98.10	11.57	128.25	123.38	22.90
AgNW-GNP4	1.48	39.62	14.69	9.67	118.43	12.88

Table 2

Characteristics of complete DSSCs based on Pt-FTO, AgNW and AgNW-GNP based counter electrodes.

CEs	GNP-loading ($\mu g/cm^2$)	V_{oc} (V)	J_{sc} (mA/cm^2)	*FF*	η (%)
Pt-FTO	–	0.58±0.01	6.47±0.26	0.44±0.01	1.87±0.15
AgNW	–	0.54±0.02	5.32±0.11	0.36±0.01	1.09±0.07
AgNW-GNP1	0.44	0.54±0.01	5.65±0.24	0.43±0.04	1.25±0.16
AgNW-GNP2	0.74	0.55±0.01	5.47±0.19	0.43±0.12	1.28±0.17
AgNW-GNP3	0.88	0.55±0.01	6.45±0.26	0.52±0.08	1.61±0.13
AgNW-GNP4	1.48	0.53±0.01	6.39±0.30	0.34±0.07	1.28±0.04

Figure Captions:

Figure 1. Schematic illustration of silver nanowire and bilayer hybrid silver nanowire-graphene nanoplatelets based counter electrodes.

Figure 2. FE-SEM images of (a) top-view of AgNW film, (b) cross-sectional tilted view of AgNW-GNP film, (c) 3D AFM images of AgNW and (d) 3D AFM images of AgNW-GNP film on glass substrate. Inset shows the higher magnification in Figure 2a and Figure 2b.

Figure 3. (a) Cyclic voltammograms, (b) Nyquist plots and (c) Tafel polarization curves of the $Co^{2+/3+}$ symmetrical cells based on Pt-FTO, AgNW, AgNW-GNP3 and AgNW-GNP4 electrodes. In Figure 3b, symbols represent the experimental data and solid lines represent the model fitting (inset).

Figure 4. (a) IPCE spectra and (b) *J-V* characteristics of DSSCs fabricated with Pt-FTO, AgNW, AgNW-GNP3 and AgNW-GNP4

Figure 1

Click here to download high resolution image

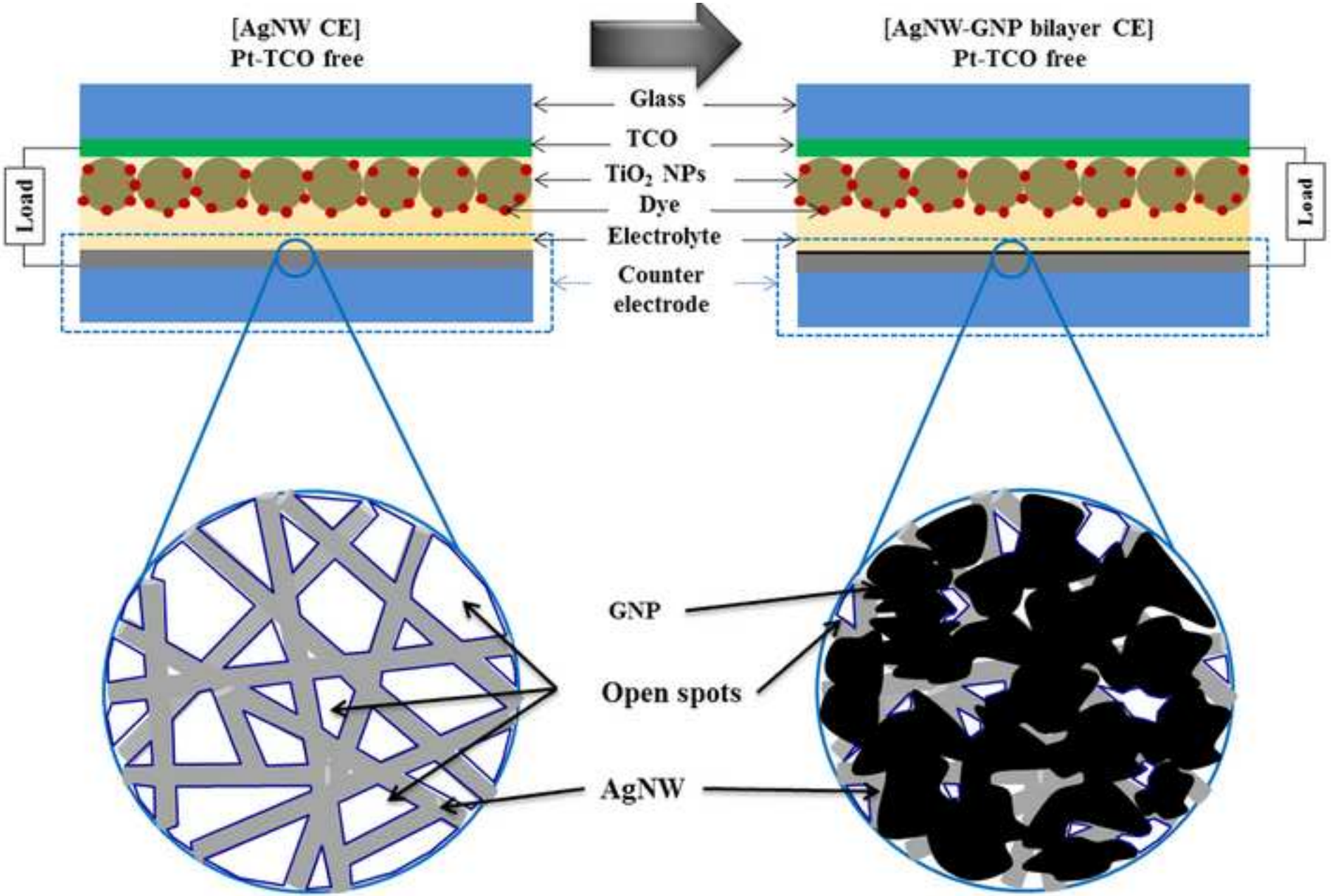

Figure 2

Click here to download high resolution image

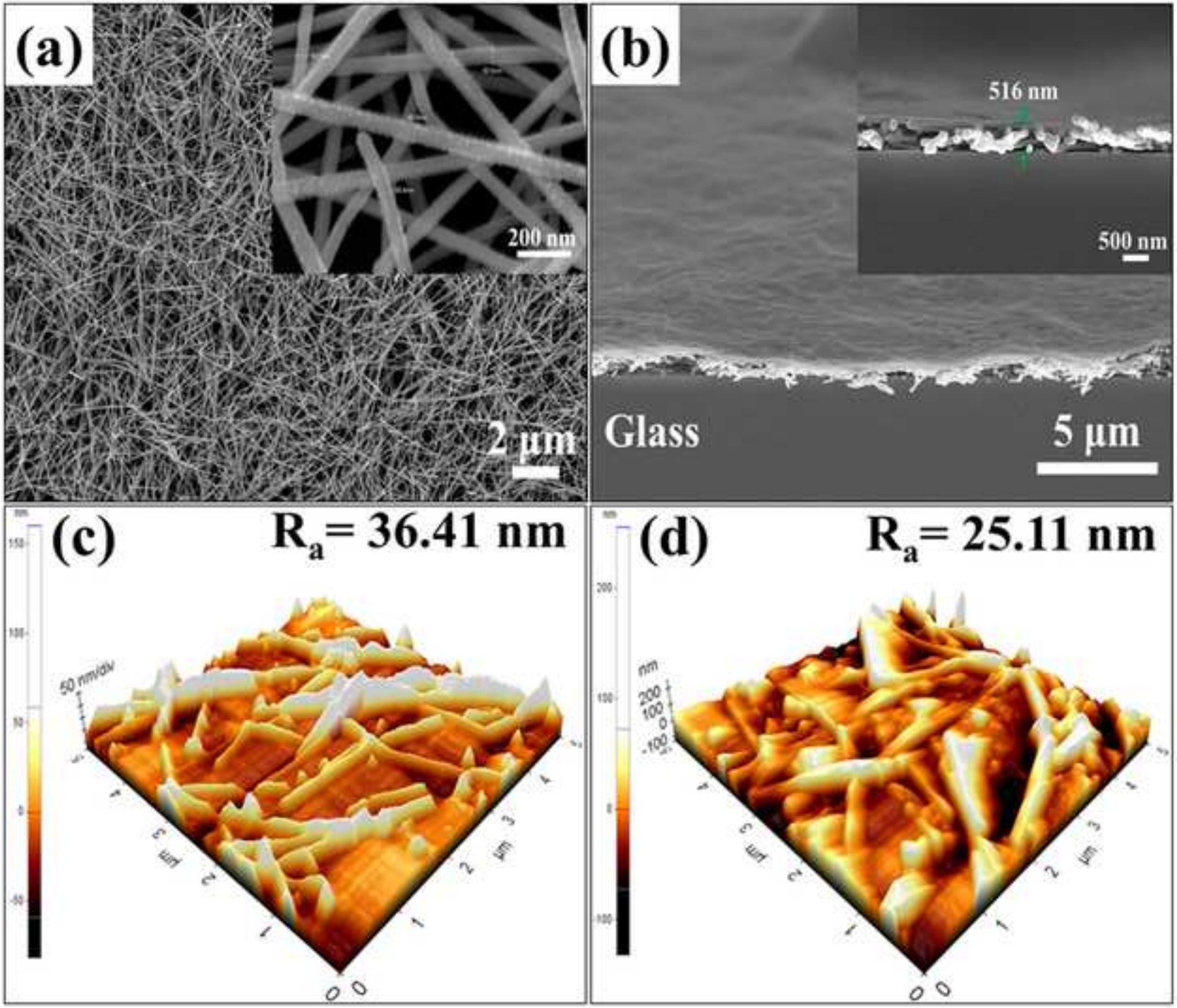

Figure 3

Click here to download high resolution image

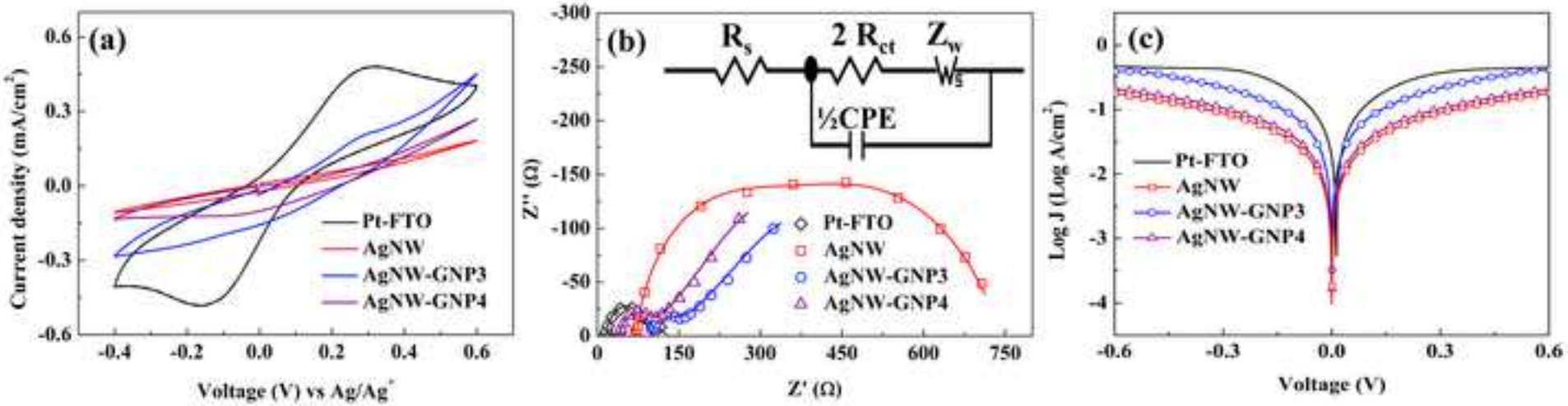

Figure 4

Click here to download high resolution image